



# Abrupt breakdown of the predictability of early season typhoon frequency at the beginning of the twenty-first century

Chao Wang<sup>1,2</sup> · Bin Wang<sup>2</sup> · Liguang Wu<sup>1</sup>

Received: 29 December 2017 / Accepted: 8 July 2018 / Published online: 17 July 2018  
© Springer-Verlag GmbH Germany, part of Springer Nature 2018

## Abstract

Maintenance of the anomalous anticyclone (cyclone) over the Philippine Sea following strong peak El Niño (La Niña) leads to a negative correlation between the pre-winter (October–December) El Niño–Southern Oscillation (ENSO) index and the tropical cyclone (TC) genesis frequency in the ensuing early TC season (January–June). This negative lead-lag correlation has established the predictability of the western North Pacific (WNP) TC genesis frequency in the early season. However, little is known about whether this relationship remains steady to date, especially in the context of evolving features of ENSO in recent decades. Here we show that the negative relationship experiences an abrupt breakdown around the early 2000s (1999–2006), which primarily occurs in the southeastern quadrant of the WNP. During the breakdown period, the anomalous anti-cyclone shifts westward to the South China Sea and an anomalous cyclonic circulation occupies the southeastern quadrant of the WNP, causing enhanced TC formation. We further reveal that the westward displacement of the WNP anticyclonic anomaly during 1999–2006 is induced by the westward shift of sea surface temperature (SST) and associated precipitation anomalies during the decaying phase of ENSO, which increases cyclonic circulation and ascending motion while reduces vertical wind shear, and thereby enhances TC formation over the southeastern WNP. The results suggest that the frequent occurrence of decaying ENSO events with SST anomaly center over the central Pacific (CP) accounts for the abrupt breakdown of predictability, and the impacts of ENSO on TC formation in the early TC season are sensitive to the location of the maximum SST anomaly. Distinguishing eastern Pacific (EP) and CP types of ENSO and/or strong and weak ENSO events may help to improve the early season TC genesis forecast over the WNP. The results also have important implications for understanding the future projection of TC changes under global warming scenarios.

## 1 Introduction

As the busiest basin of tropical cyclone (TC) activity, the western North Pacific (WNP) experiences about 26 TCs per year (e.g., Gray 1968; Chan 2005). The TC-induced gale winds, heavy precipitation, storm surges and landslides can cause enormous socio-economic disasters to billions of people in the Pacific Islands and Asian coastal countries (Zhang

et al. 2009). Therefore, seasonal forecasting of TC activity is key to minimizing the losses brought by TC-induced disasters (Camargo et al. 2007; Zhan et al. 2012).

El Niño–Southern Oscillation (ENSO) is a primary predictability source of the inter-annual variability of TC activity (e.g., Chan et al. 1998, 2001; Wang and Chan 2002; Zhan et al. 2012). A number of studies suggested that the inter-annual variability of TC activity over the WNP is closely related to ENSO (e.g., Chan 1985, 2000; Lander 1994; Wang and Chan 2002; Camargo and Sobel 2005; Zhao et al. 2011; Wang et al. 2013a, b, 2018c; Wang and Wu 2016). There is a general consensus that El Niño shifts TC formation locations southeastward during its developing phase (e.g., Chen et al. 1998; Chan 2000; Chia and Ropelewski 2002; Wang and Chan 2002) by extending the low-level monsoon trough and shifting the tropical upper-tropospheric trough eastward (e.g., Chia and Ropelewski 2002; Wang and Chan 2002; Wu et al. 2015; Wang and Wu 2016, 2018a, b). As a result of the southeastward displacement of TC formation, TCs tend

✉ Bin Wang  
wangbin@hawaii.edu

<sup>1</sup> Key Laboratory of Meteorological Disaster of Ministry of Education, Joint International Research Laboratory of Climate and Environment Change, Collaborative Innovation Center on Forecast and Evaluation of Meteorological Disasters, Nanjing University of Information Science and Technology, Nanjing, China

<sup>2</sup> Department of Atmospheric Sciences and International Pacific Research Center, University of Hawaii at Manoa, 2525 Correa Rd., Honolulu, HI 96822, USA

to have stronger intensity due to the prolonged stay over the tropical warm ocean (e.g., Wang and Chan 2002; Camargo and Sobel 2005; Zhao et al. 2011).

During the decaying phase, El Niño conveys its impact to Asian climate through the anomalous Philippine Sea anticyclone (PSAC), which is maintained by a local positive feedback between atmospheric Rossby waves and ocean mixed-layer thermodynamics (e.g., Wang et al. 2000, 2003, 2013a). The anomalous PSAC can affect the large-scale conditions which are important to TC formation, and thus suppress TC formation over the WNP. As a result, TC counts tend to decrease in the early TC season following strong El Niño events. In contrast, during the La Niña decaying phase, an anomalous cyclonic circulation over the WNP can prompt TC formation in the early season (Wang and Chan 2002). Based on this well-known physical understanding, Wang and Chan (2002) established an empirical scheme to predict the TC counts in the following early season (January–June) by using the pre-winter (OND) Niño 3.4 index which shows considerable prediction skill.

However, the data they used to establish the predictability is from 1965 to 1999. Now 17 years have already passed, and it is unknown whether the relationship between the peak ENSO and the TC genesis frequency in the ensuing early TC season remains valid. This motivates us to examine possible changes in the predictability of early season TC frequency, and we find that an abrupt breakdown of this predictability occurred in the early 2000s. In this study, we first document this abrupt change and then explain the underlying mechanism that causes the breakdown. The understanding gained from this analysis will provide further guidance for improving seasonal prediction.

The remainder of this paper is organized as follows. Section 2 describes the data adopted in this study, while the abrupt breakdown in the predictability in the early 2000s is presented in Sect. 3. Section 4 compares the ENSO-related large-scale conditions between 1965–1998 and 1999–2006. The underlying mechanism related to the abrupt breakdown in predictability is discussed in Sect. 5. Section 6 presents a summary.

## 2 Data and method

Best track datasets from the Joint Typhoon Warning Center (JTWC) and the Regional Specialized Meteorological Centre (RSMC) Tokyo-Typhoon Center of Japan Meteorological Agency (JMA) are used to obtain TC information. TCs are defined as those in the dataset whose maximum wind speed reaching tropical storm intensity ( $17.2 \text{ ms}^{-1}$ ). The monthly wind, humidity and precipitation from NCEP–NCAR Reanalysis dataset (Kalnay et al. 1996) are adopted to derive the large-scale environments. Monthly sea surface temperature

(SST) from version 4 of the National Oceanic and Atmospheric Administration Extended Reconstructed SST (ERSST) dataset (Huang et al. 2015) is used to demonstrate SST evolutions associated with ENSO.

The analysis period in this study is from 1965 to 2016. The year 1965 is selected as the starting year because routine satellite coverage began around this year (e.g., Chan 2006; Wang and Wu 2012). In this study, we focus on the relationship between the preceding pre-winter ENSO represented by the October, November and December (OND) mean Niño 3.4 index and the subsequent early season (January–June) TC genesis number. The definition of the TC activity season is consistent with the previous studies (e.g., Wang and Chan 2002; Hsu et al. 2014; Wang and Wu 2015). Correlation, regression, and Empirical Orthogonal Function (EOF) analyses are employed to present the results and a statistical significance level is assessed using the two-tailed Student's *t* test (Wilks 2011).

## 3 Abrupt breakdown of the peak ENSO-early TC genesis relationship in the early 2000s

The WNP TC frequency in the early TC season experiences considerable inter-annual variability (Fig. 1). For instance, 11 TCs are formed in 1965, 1971 and 2004, while none come into existence in 1973, 1998 and 2016. One may note that these extremums are generally related to the ENSO events except in 2004. Actually, the TC frequency in the early TC season has a significant negative correlation with the OND Niño 3.4 index during 1965–2016 (correlation coefficient  $r = -0.48$ ,  $p < 0.01$ ). Compared to the results in Wang and Chan (2002), however, the correlation coefficient reduces

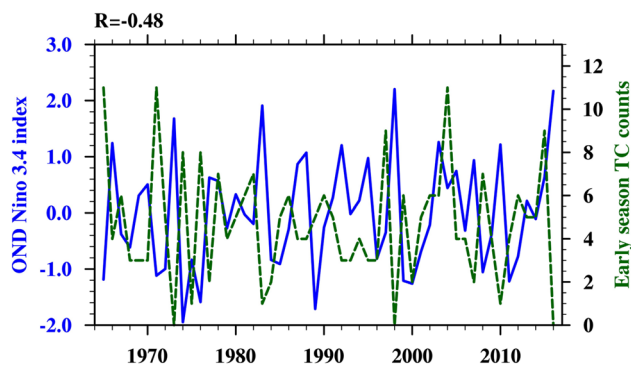


**Fig. 1** Time series of OND(0) Niño 3.4 index (blue solid line) and TC counts in the following early season [January(1)–June(1), green dash line] over 1965–2016. Correlation is shown in the top left of the panel. Numerals in the parentheses denote years relative to El Niño: 0 for its developing year and 1 for decaying year

significantly. Adding the new records from 2000 to 2016 causes the decreasing negative correlation.

Figure 2a shows a 21-year running mean correlation coefficient between the OND Niño 3.4 index and the TC genesis number in the ensuing early TC season from two best track datasets. It looks like that the relationship suddenly changes in the mid-1990s from statistically significant to insignificant at the 95% confidence level, which seems to suggest an interdecadal change of the relationship. However, this is not the case.

Carefully inspecting the time series in Fig. 1, we find that the negative correlation breaks down only in an 8-year period from 1999 to 2006 (the shaded period in Fig. 2). In fact, the correlation for 1965–1998 is  $-0.6$ , but it turns to a positive value ( $r = 0.39$ ) during 1999–2006. However, the negative correlation recovers to  $-0.6$  during the period of 2007–2016, suggesting that the ENSO-related predictability only breaks down in the early 2000s (Fig. 2b). Therefore, one should be cautious about detection of decadal change using long-period running means as it may lead to a deceptive conclusion.

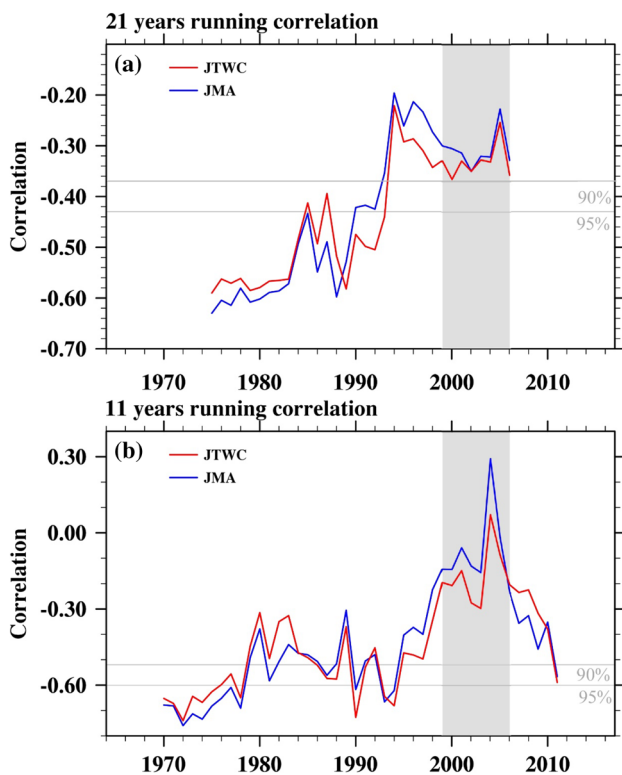


**Fig. 2** The running correlations between the OND Niño 3.4 index and TC genesis number in the following early season from JTWC (red curves) and JMA (blue curves) best track datasets with **a** 21-year and **b** 11-year running windows. The horizontal solid lines denote the 90 and 95% significant levels. The gray bars highlight the breakdown period

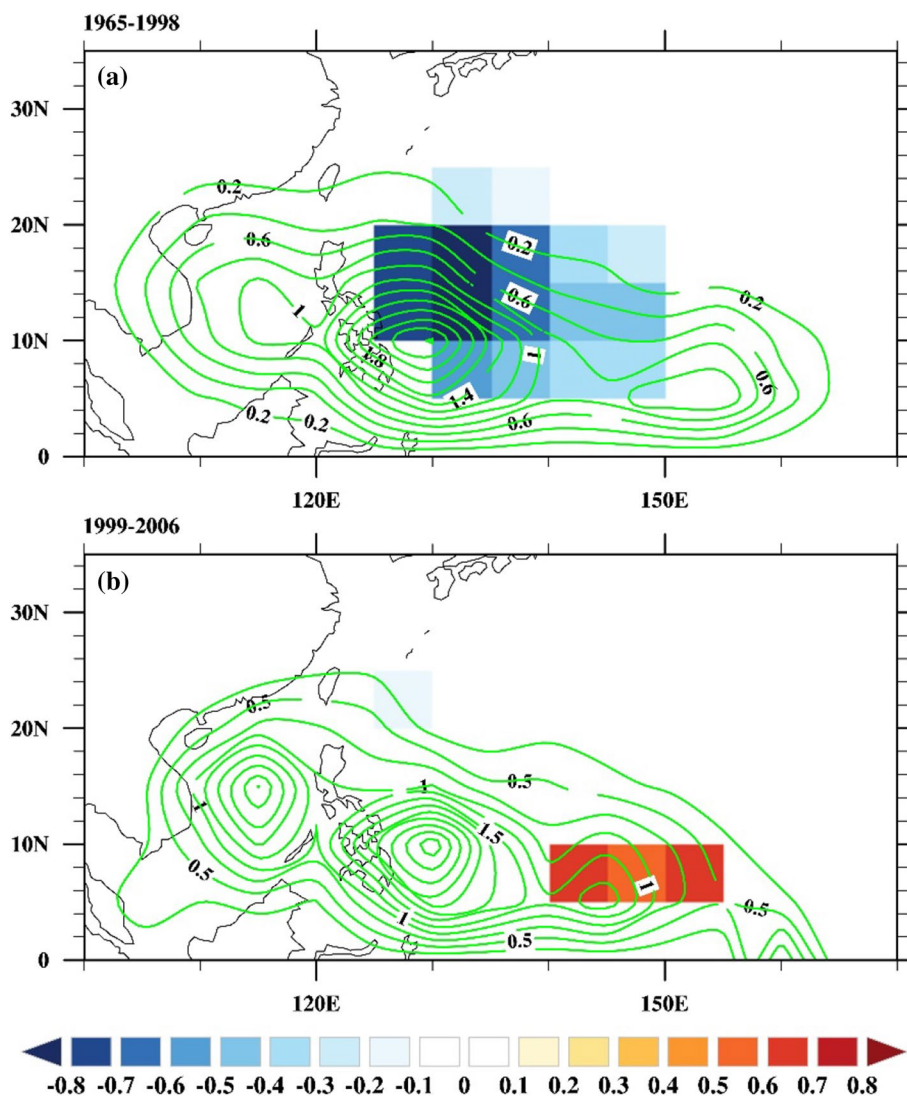
To understand the cause of the abrupt breakdown, in the following analyses we compare the ENSO-related TC statistics and large-scale conditions during 1999–2006 to those of 1965–1998. We also compared the ENSO-related TC statistics and large-scale conditions during 1999–2006 to those of 2007–2016, it is found that the results are generally similar. Actually, the abrupt breakdown is mainly attributed to the TC formation during April–June (AMJ, Figure not shown), so we focus on AMJ in the following analyses to pinpoint the prominent features of TC formation and large-scale conditions related to this abrupt breakdown.

Climatologically, AMJ TC genesis mostly occurs to the south of  $20^{\circ}\text{N}$ , and is distributed along a northeast–southwest tilted zone extending from the South China Sea to the tropical eastern WNP with a maximum at  $10^{\circ}\text{N}$ ,  $130^{\circ}\text{E}$  (Fig. 3). The distribution coincides with that of favorable large-scale circulations in this region (e.g., Briegel and Frank 1997; Ritchie and Holland 1999). One should note that the TC formation over the eastern WNP is suppressed due to the westward migration of the tropical upper-tropospheric trough during 1999–2006 (Wu et al. 2015). In the first epoch (1965–1998), the composite difference in TC genesis frequency between positive and negative OND Niño3.4 years displays negative anomalies east of  $120^{\circ}\text{E}$  (Fig. 3a), which is in accordance with suppressed TC formation following El Niño events (Wang and Chan 2002). In contrast, for the period of 1999–2006, the composite TC frequency difference shows prominent positive anomalies in the southeastern WNP (Fig. 3b). It is clear that the abrupt breakdown during 1999–2006 is primarily attributed to the abnormal TC formation over the southeast quadrant of the WNP (east of  $135^{\circ}\text{E}$  and south of  $20^{\circ}\text{N}$ ) illustrated in Fig. 3a, b. As the results derived from the JTWC and JMA data are generally similar, only the findings based on the JTWC best track data are presented in the following analyses.

#### 4 Contrast of ENSO-related large-scale conditions in the two epochs

Thermodynamic and dynamic large-scale conditions, such as vertical wind shear, low-level vorticity, mid-level humidity, vertical motion and so on, play an essential role in TC formation (e.g., Gray 1968; Emanuel and Nolan 2004; Murakami and Wang 2010). Thus, examination of large-scale conditions helps to gain insight into the cause of the distinct features of ENSO-related TC formation over the southeast WNP in the two epochs (Figs. 4, 5). In the first epoch (1965–1998), the ENSO-related 850 hPa relative vorticity is generally negative to the south of  $20^{\circ}\text{N}$ , suppressing TC formation. Additionally, the anomalous descending motion south of  $20^{\circ}\text{N}$  is also unfavorable for TC formation (Fig. 4a). In terms of zonal vertical shear

**Fig. 3** Spatial distribution of AMJ TC formation climatology (contours, number decade<sup>-1</sup>) and composite TC genesis frequency difference between positive and negative OND Nino3.4 years (shadings, number decade<sup>-1</sup>) at each 5° latitude × 5° longitude box for **a** 1965–1998, and **b** 1999–2006. Shadings represent the values above the 90% confidence level



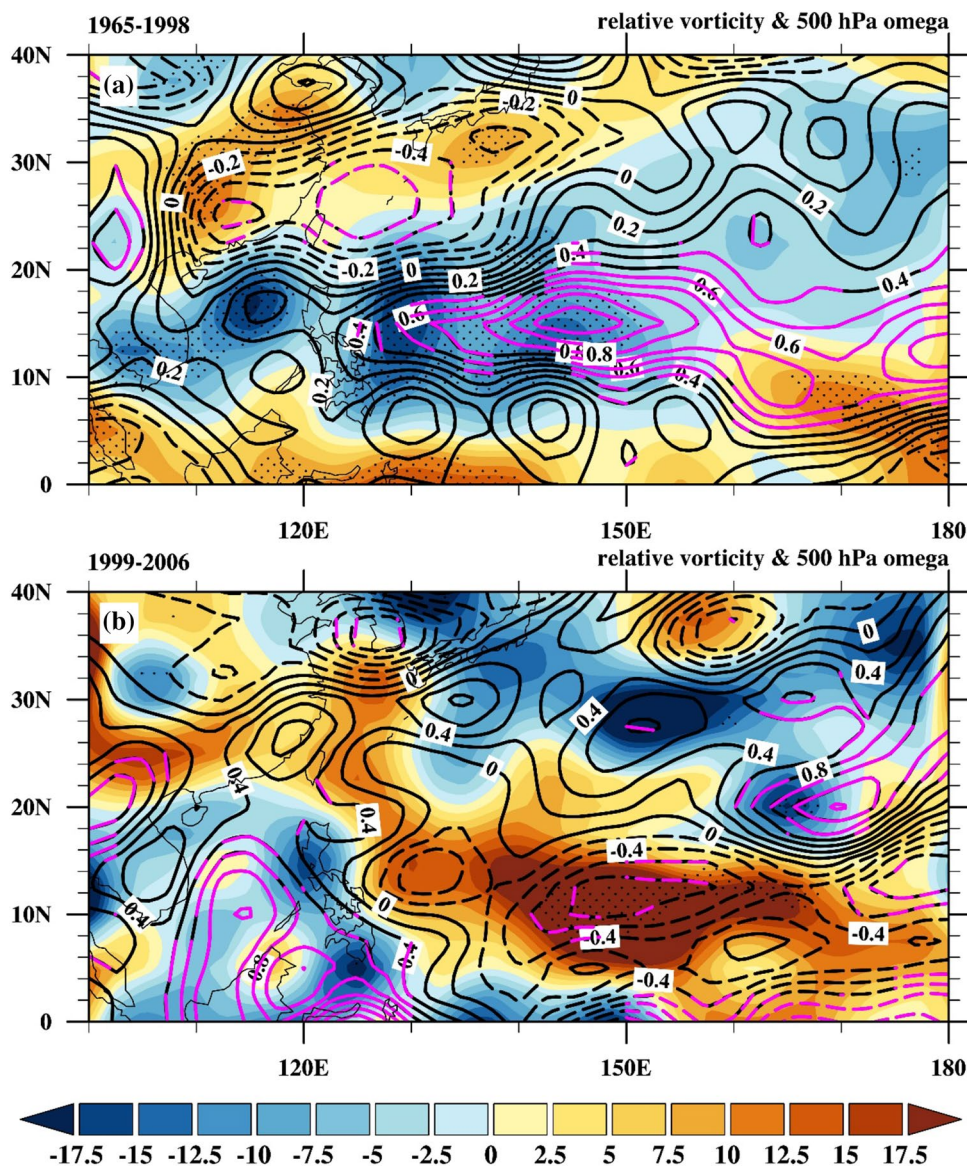
and 700 hPa relative humidity, the enhanced vertical shear and decreased mid-level humidity serve to suppress TC formation as well (Fig. 5a). These unfavorable large-scale condition anomalies related to ENSO are in accordance with suppressed TC formation during 1965–1998, as illustrated in Fig. 3a. In the second epoch, the large-scale conditions during an ENSO decaying phase are remarkably different from those in the first epoch (Figs. 4b, 5b). The most prominent difference is located in the southeast quadrant of the WNP. All the large-scale conditions in the southeast quadrant of the WNP, including positive vorticity anomalies, anomalous rising motion, moistening of the mid-troposphere and decreased vertical shear, promote TC formation (Figs. 4b, 5b). The favorable large-scale conditions well match enhanced TC formation in the southeast WNP during 1999–2006, as illustrated in Fig. 3b. The coherence between the anomalous TC formation and large-scale conditions indicates that changes

in the large-scale environments are contributed to the reversed ENSO-TC relationship in the two epochs.

## 5 Possible mechanism for the reversed ENSO-TC relationship

To understand the causes of the contrasting large-scale circulation conditions during the two epochs, we turn attention to the lower boundary SST anomalies. Normally, after a strong El Niño matures during the northern winter, a low-level anticyclonic anomaly dominates the Philippine Sea (Wang et al. 2000), which produces descending motion and low-level anticyclonic vorticity and dries the lower troposphere, thus suppressing TC genesis and leading to a negative ENSO-TC relationship. This Philippine anticyclone emerges in the autumn (SON) of the El Niño developing year and reaches a peak and persists in the ensuing winter and spring (Wang

**Fig. 4** Regressed AMJ 850 hPa relative vorticity (shadings,  $10^{-7} \text{ s}^{-1}$ ) and 500 hPa omega (contours,  $10^{-2} \text{ Pascal s}^{-1}$ ) anomalies with respect to OND Niño 3.4 index for **a** 1965–1998, and **b** 1999–2006. The stippling and magenta contours denote areas that are significant at the 90% confidence level

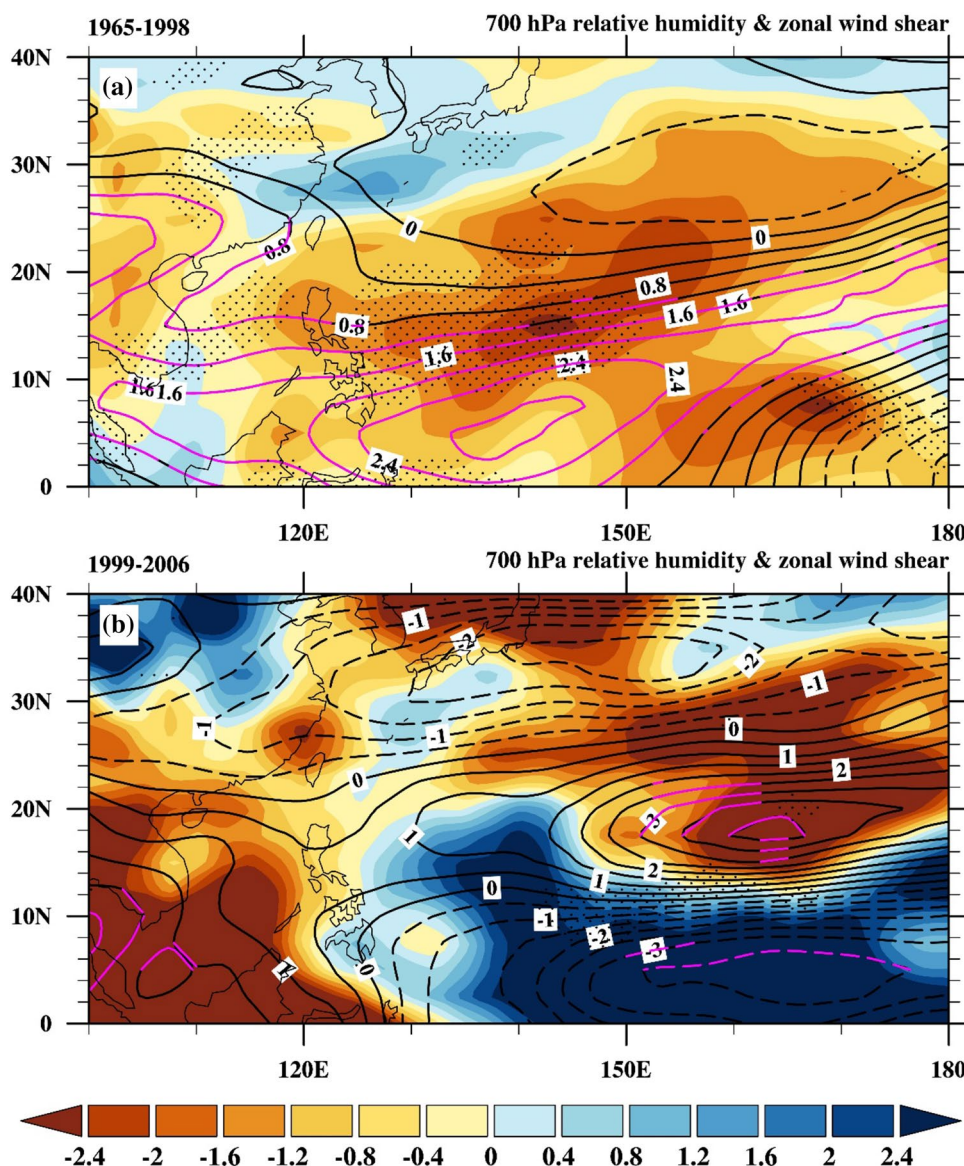


and Zhang 2002). This evolution process is what we see in Fig. 6a–c for the first epoch.

Figure 6 compares the evolutions of ENSO-related circulations and underlying SST anomalies for the two epochs. The ENSO-regressed SST in OND (0) exhibits a typical El Niño pattern over the Pacific in both epochs. Namely, prominent warming anomalies occur in the equatorial central-eastern Pacific and cooling anomalies occupy the western equatorial and subtropical Pacific (Fig. 6a, d). In response to the SST anomalies, the ENSO-regressed precipitation and upper-level velocity potential display a dipole pattern over the Pacific due to the weakening Walker circulation. That is to say, enhanced ascending motion and precipitation occur in the central-eastern Pacific, while suppressed ascending motion and precipitation appear over the Maritime Continent (Fig. 7a, d). As a direct Rossby wave response to the

positive heating anomalies over the central-eastern Pacific, a cyclonic pair symmetric about the equator extends to the eastern Pacific (EP). The northern part of the cyclonic pair shifts TC formation southeastward over the WNP (Wang and Chan 2002). Meanwhile, the anomalous anticyclone (i.e. PSAC) occurs west of 120°E as a Rossby wave response to the negative heating over the Maritime Continent. Note that in the first epoch, when the cyclonic circulation east of 140°E weakens and shifts to the EP due to the decaying warming, the anomalous PSAC extends eastward in JFM(1) and maintains to AMJ(1) by a positive local thermodynamic air–sea feedback (Fig. 7a–c, e.g., Wang et al. 2000, 2003). The anomalous PSAC and negative precipitation anomalies tend to suppress TC formation, which is consistent with the negative correlation in Wang and Chan (2002). During the later epoch, however, the anticyclonic anomaly does not

**Fig. 5** Regressed AMJ 700 hPa relative humidity (shadings, %) and zonal wind shear ( $\text{m s}^{-1}$ ) anomalies with respect to OND Niño 3.4 index for **a** 1965–1998, and **b** 1999–2006. The stippling and magenta contours denote areas that are significant at the 90% confidence level



move eastward but remains in the South China Sea from OND(0) to AMJ(1). Meanwhile, an anomalous cyclonic circulation, as a direct Rossby wave response to the anomalous convective heating over the central equatorial Pacific, persists from OND(0) to AMJ(1) over the Philippine Sea (Fig. 7d–f). Persistence of this anomalous cyclonic circulation into AMJ(1) contributes to enhanced TC formation in the southeastern WNP in the later epoch.

The question is why in the first epoch the AC anomaly moves from the South China Sea to the Philippine Sea, whereas in the second epoch it does not. Comparing the SST anomaly evolution in the two epochs (Fig. 6), we find that this difference is related to the different El Niño decay processes in the two periods. Although the SST warming patterns during OND(0) are similar in the two epochs, in JFM (1), the El Niño anomalies in the first epoch retreat

eastward with a maximum warming center located at  $140^{\circ}\text{W}$ , while the SST anomalies in the second one are centered at  $165^{\circ}\text{W}$ , about  $25^{\circ}$  longitudes to the west. During AMJ(1), SST anomalies of both epochs weaken but the warming center is located at  $140^{\circ}\text{W}$  in the first epoch while near the dateline at the central Pacific (CP) in the second epoch. This indicates that in the first epoch El Niño evolves into an EP type of El Niño, whereas in the latter it evolves into a CP type of warming.

The difference in the SST distribution can be clearly seen from Fig. 8a, which shows the zonal structures of the regressed AMJ(1) SST anomalies averaged over the equatorial band ( $5^{\circ}\text{S}$ – $5^{\circ}\text{N}$ ) in the two epochs. Evidently, SST anomalies of decaying El Niño exhibit a westward shift during the later epoch. The westward displacement of SST anomalies further “pushes” the precipitation heating

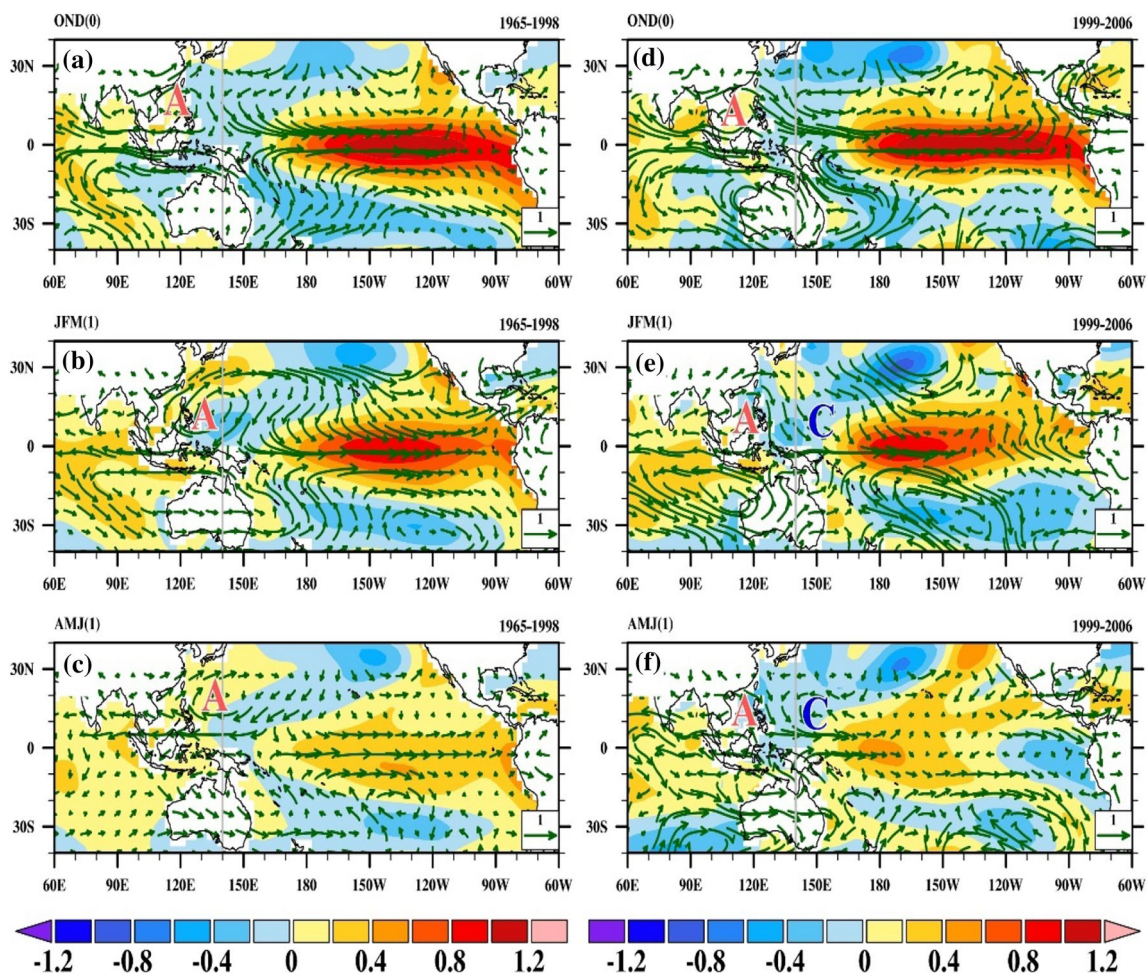


**Fig. 6** Seasonal evolutions from OND (0) to AMJ (1) of regressed SST (shading) and 850 hPa wind anomalies for 1965–1998 (a–c) and 1999–2006 (d–f) with respect to OND Niño 3.4 index. The numer-

als in parentheses denote the ENSO developing (0) and decaying (1) years. The grey lines denote 140°E. A denotes the anti-cyclonic circulation and C denotes the cyclonic circulation

anomalies (Fig. 8b) and the corresponding 200 hPa velocity potential (upper-level divergence) anomalies (Fig. 8c) westward. In particular, the westward shift of SST warming stimulates a cyclonic circulation anomaly over the southeastern WNP as a direct Rossby wave response, which leads to the reversed ENSO-TC relationship in the later epoch.

The westward shift of ENSO-related heating and circulations is thought to be related to the frequent occurrence of the CP-type El Niño in the early 2000s (e.g., Larkin and Harrison 2005; Ashok et al. 2007; Kao and Yu 2009; Kug et al. 2009; Yeh et al. 2009; Xiang et al. 2013). Additionally, SST warming in the CP has a relatively longer developing period and more persistence than that in the EP (e.g., McGregor et al. 2012; Xiang et al. 2013).

Figure 9a, b shows that the leading mode of the tropical Pacific SST anomaly has changed in the early 2000s with its maximum center shifting westward. The westward shift of the anomalous zonal wind stress and precipitation can also be found in the regressed pattern against the

principal component of the first leading mode in the second epoch (Fig. 9c, d). Actually, the events of 2001–2002, 2002–2003 and 2004–2005 are categorized as the CP-type El Niño events (Yeh et al. 2009). Although the definition of CP-type of El Niño is described with large diversity, SST maximum centers can be found in the CP in these events. Even in the 2003–2004 event, there is an SST extremum in the CP although it usually identified as an EP El Niño due to the greater SST warming magnitude over the EP (figure not shown). The SST anomalies during 1999–2000 and 2000–2001 also show negative SST anomaly centers over the central equatorial Pacific (Wang et al. 2013b). These results reflect the fact that the frequent occurrence of ENSO events with SST anomaly centers over the CP accounts for the abrupt breakdown of predictability in the early 2000s.

Due to the short duration of the second epoch, one may wonder whether the findings are robust. To confirm the robustness of the results, we take more cases into account by using historical records. It should be noted that the

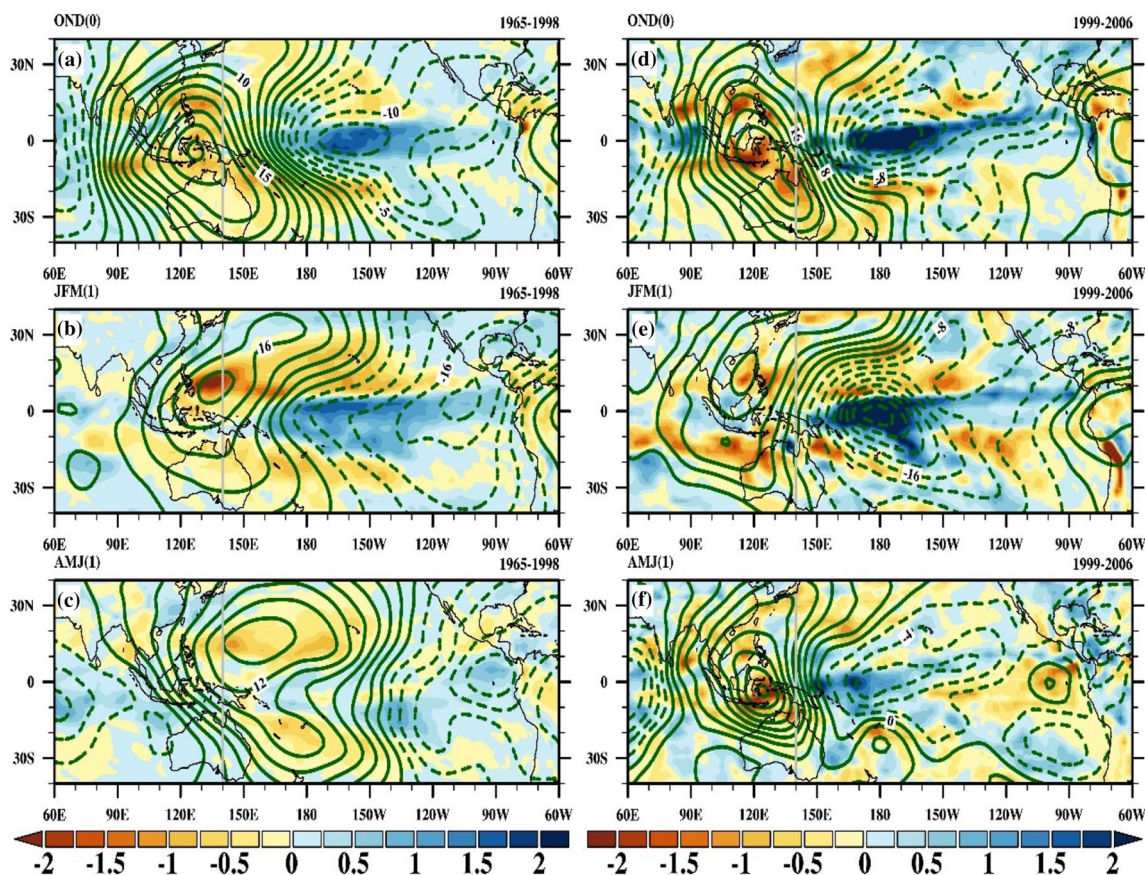


**Fig. 7** Same as Fig. 6 but for surface precipitation (shadings,  $\text{mm day}^{-1}$ ) and 200 hPa velocity potential (contours,  $10^5 \text{ m}^2 \text{ s}^{-1}$ )

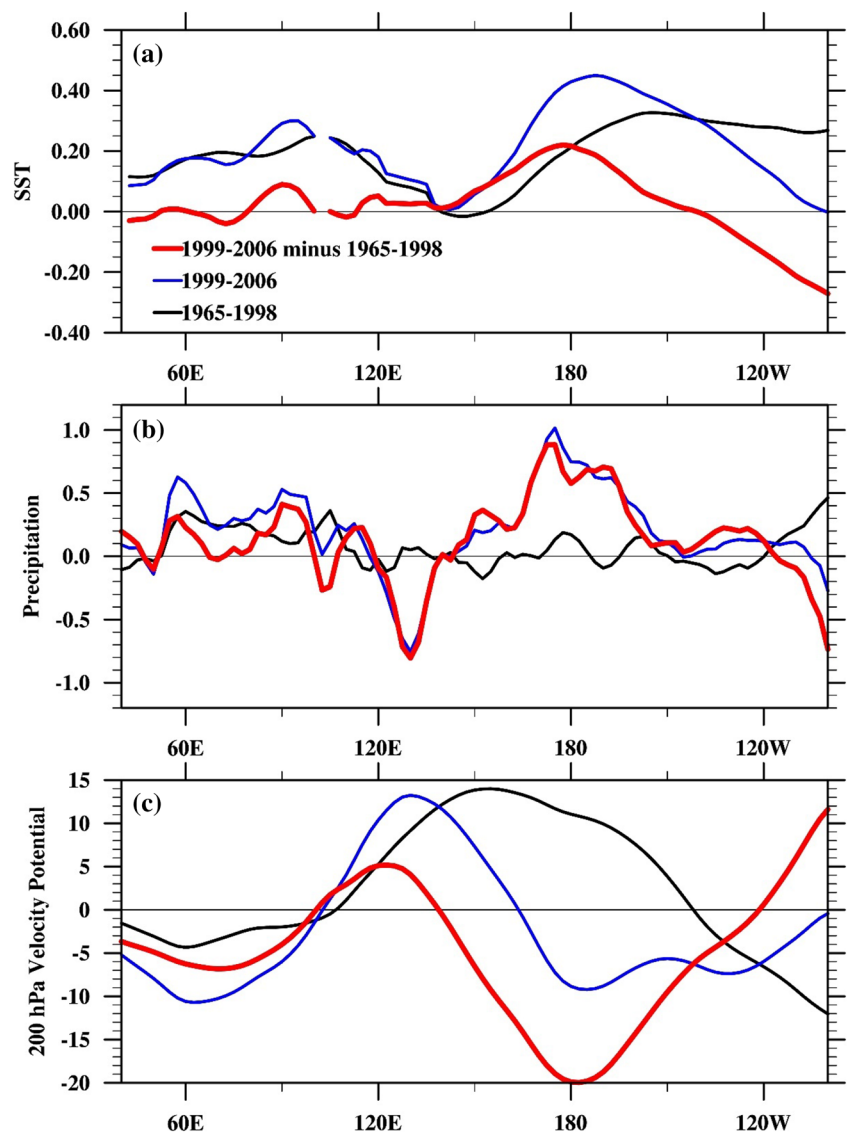
relationship between the OND Niño 3.4 index and TC counts in the following early season displays considerable inter-annual variability (Fig. 10). More specifically, in some years TC formation over the WNP is above (below) normal following El Niño (La Niña) event, as illustrated in the first (third) quadrant of Fig. 10.

Examining the reversed relationship in individual years helps to gain insight into the mechanism governing TC formation in the early season. Figure 11 shows the evolution of regressed SST and 850 hPa wind anomalies in years with negative and positive correlation respectively. For negatively correlated years (Fig. 11a–c), cyclonic circulation anomalies over the WNP in OND(0) change to anticyclonic circulation anomalies during JFM(1) and AMJ(1), which results in the negative relation between the Niño 3.4 index and early season TC frequency. In contrast, for positive correlation years (Fig. 11d–f), the anomalous cyclonic circulation over the WNP in OND(0) can persist to the decaying phase, leading to enhanced TC formation in the early season. The evolutions of SST and 850 hPa winds in the two groups are basically consistent with those shown in Figs. 7 and 8. In the negative correlation cases, the

maximum center of El Niño SST warming is located at the eastern equatorial Pacific, and the anomalous cyclonic circulation changes to an anomalous anticyclonic circulation over the WNP due to the local air-sea interaction as the EP SST warming dissipates (e.g., Wang et al. 2000, 2003). In a similar way, anomalous anti-cyclonic circulation changes to an anomalous cyclonic circulation over the WNP in the early season following La Niña events. However, the SST warming (cooling) of El Niño (La Niña) shifts westward and persists to AMJ (1) in the positive correlation group. As a result, the cyclonic (anti-cyclonic) circulation over the WNP, as a Rossby wave response to enhanced (suppressed) convective heating in the CP region, persists from OND (0) to AMJ (1) and further leads to enhanced (suppressed) TC formation. Previous studies found that the El Niño and La Niña are not a simple mirror image (Meinen and McPhaden 2000; Okumura and Deser 2010). Therefore, the asymmetry in El Niño and La Niña should be considered when interpreting the results for a specific ENSO event. In view of these results, we consider the westward shift in SST and precipitation anomalies as the main cause of the abrupt breakdown of predictability in the early 2000s.



**Fig. 8** The 5°S–5°N averaged zonal structures for regressed AMJ anomalies of **a** SST (K), **b** precipitation (mm day<sup>-1</sup>) and **c** 200 hPa velocity potential (10<sup>5</sup> m<sup>2</sup> s<sup>-1</sup>) during 1999–2006 (blue solid lines) and 1965–1998 (black solid lines) with respect to OND Niño 3.4 index. The difference between 1999–2006 and 1965–1998 is shown by red solid lines



## 6 Summary

### 6.1 Conclusion

After a strong El Niño matures during the northern winter, a low-level anticyclonic anomaly dominates the Philippine Sea (Wang et al. 2000), which produces descending motion and low-level anticyclonic vorticity and dries the lower troposphere, thus suppressing TC genesis over the WNP (Wang and Chan 2002). This Philippine anticyclone emerges in the autumn (September–November) of the El Niño developing year and reaches a peak and persists in the ensuing winter and spring (Wang and Zhang 2002; Lau and Nath 2003; Lau et al. 2004). The opposite is true for strong La Niña events. The anomalous anti-cyclone (cyclone) over the Philippine Sea following strong El Niño (La Niña) event, which is maintained by the air-sea interaction, leads to the negative

relationship between the peak ENSO index and the TC genesis frequency in the ensuing early TC season (January–June) (Wang and Chan 2002). The negative lead-lag correlation between OND (October–December) Niño 3.4 index and TC genesis frequency in the ensuing early TC season (January–June) has established the seasonal predictability of the WNP TC frequency in the early season.

However, we find that the negative ENSO-early TC relationship experiences an abrupt breakdown at the turn of the twenty-first century, as revealed by analyses of the historical best track datasets from JTWC and JMA. More specifically, the correlation for 1965–1998 is  $-0.6$ , but it turns to positive ( $r=0.39$ ) during 1999–2006 and then returns to  $-0.6$  during 2007–2016. This abrupt breakdown of the negative correlation in the early 2000s mainly occurs in the southeastern quadrant of the WNP, which is in accordance with the anomalous large-scale conditions in this region during the

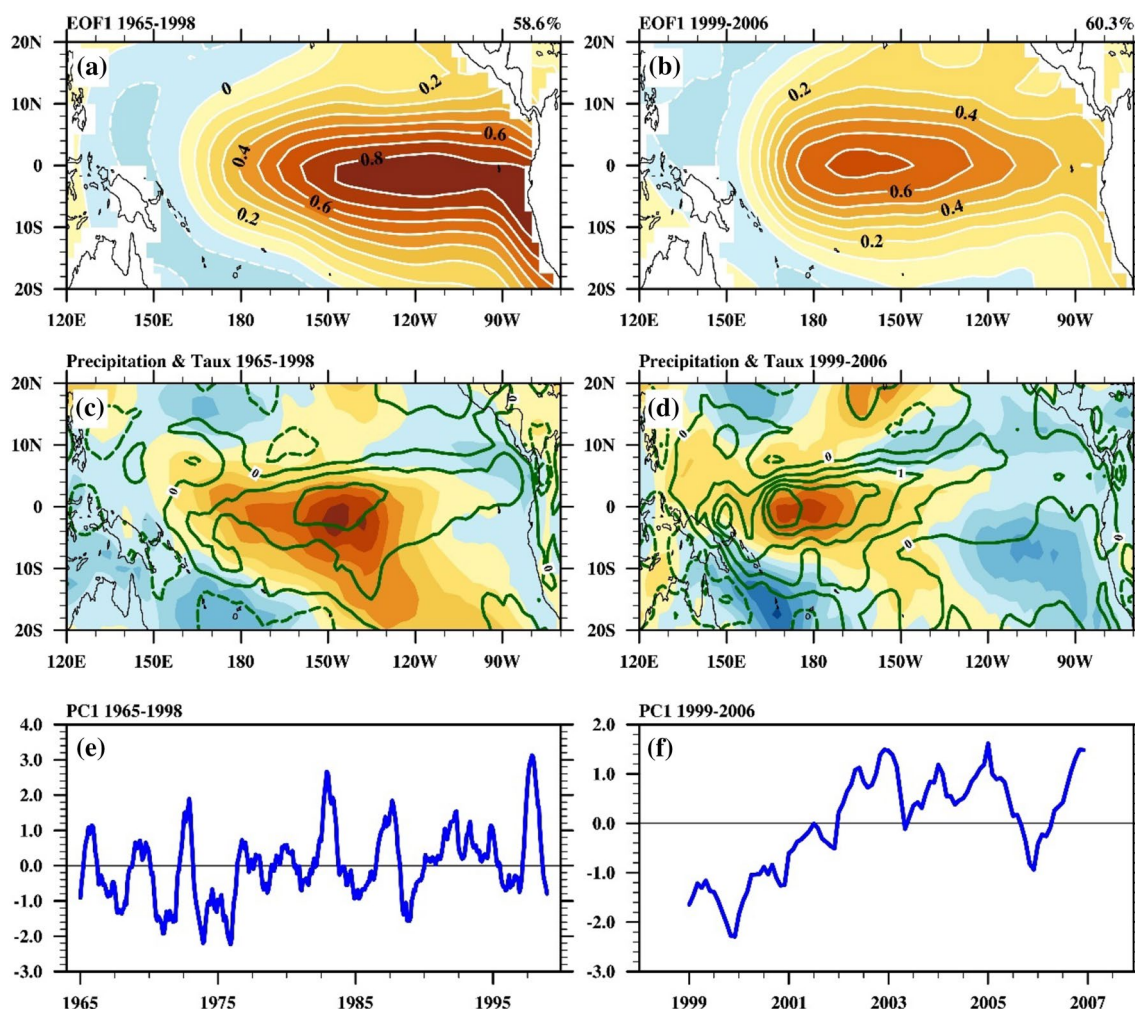


**Fig. 9** The leading EOF mode of monthly mean SST anomalies over the tropical Pacific during **a** 1965–1998 and **b** 1999–2006. The fractional variance that can be explained by the EOF-1 mode is 58.6 and 60.3%, respectively. The corresponding principal components are

shown in **e** and **f**. Regressed precipitation anomaly (contours,  $\text{mm day}^{-1}$ ) and surface zonal wind stress anomaly (shadings,  $\text{dyn cm}^{-2}$ ) with respect to the corresponding principal component of leading EOF during **c** 1965–1998 and **d** 1999–2006

ENSO decaying phase. The westward shift of SST anomalies in the decaying phase of ENSO and the associated westward displacement of convective heating anomalies during 1999–2006 are found to be responsible for creating these favorable anomalous large-scale conditions for TC genesis, including the low-level vorticity, 500 hPa vertical motion and vertical wind shear.

During 1965–1998, the maximum center of ENSO-decaying SST and precipitation is generally located in the eastern equatorial Pacific ( $140^{\circ}\text{W}$ ), and these anomalies gradually dissipate in the following early season. Meanwhile, an anticyclonic anomaly, which is established in the fall of the El Niño developing year, extends eastward from the South China Sea to the Philippine Sea and is then maintained until early summer by the local thermodynamic air–sea feedback (e.g., Wang et al. 2000, 2003). The opposite is true for La Niña events. The anticyclonic

(cyclonic) circulation over the WNP following El Niño (La Niña) events leads to a negative relationship between the OND Niño 3.4 and TC frequency in the following early season.

In contrast, during 1999–2006, the ENSO-related SST and precipitation anomalies shift westward to the CP during the ENSO decaying phase and persist into the following early TC season. After an El Niño matures, positive CP heating anomalies directly excite an anomalous cyclonic circulation over the WNP, which persists from OND(0) to AMJ(1) and further induces enhanced TC formation in the WNP. The circulations are opposite during La Niña events, leading to suppressed early season TC formation in the WNP. It is discovered that the frequent occurrence of ENSO events with SST anomaly center over the CP mainly accounts for the abrupt breakdown of predictability in the early 2000s.

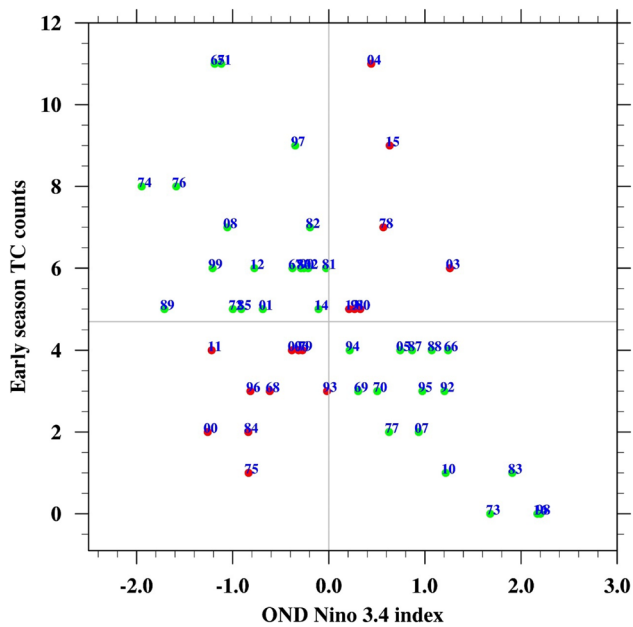


**Fig. 10** Scatter plot of the early season TC genesis frequency and OND Niño 3.4 index over 1965–2016. The numbers denote the calendar year. Red (green) dots indicate the years with positive (negative) correlation between the early season TC frequency and OND Niño 3.4 index

## 6.2 Discussion

Results of this study suggest that the impacts of ENSO on TC formation in the following early season are sensitive to the location and persistence of the maximum SST anomaly and the associated precipitation anomaly, because the different location of heating source may produce reversed circulations as well as large-scale conditions over the southeastern WNP.

Some recent studies introduced a new type of El Niño whose maximum warming is located at the equatorial CP (e.g., Larkin and Harrison 2005; Weng et al. 2007; Kao and Yu 2009; Kug et al. 2009; Yeh et al. 2009; Xiang et al. 2013). It is different from the canonical El Niño, as the latter's maximum warming is in the EP. Compared with the EP El Niño, the CP-type El Niño exerts different impacts

on global climate (e.g., Ashok et al. 2007; Weng et al. 2007, 2009) as well as TC activity (Kim et al. 2009, 2011; Chen and Tam 2010; Hong et al. 2011; Wang et al. 2013a, b). For instance, Chen and Tam (2010) revealed that the CP El Niño index is significantly correlated with the TC frequency during the ENSO developing summer over the WNP, while no significant correlation is found if one uses the EP El Niño index. Kim et al. (2011) found that TC activity over the WNP is sensitive to the location of ENSO-induced heating. These studies pay attention to the different impacts of the two types of El Niño on TC activity in the ENSO developing phase. Our study shows the impacts of the CP El Niño on TC genesis in the El Niño decaying phase, which can cause the breakdown of the negative OND ENSO-early TC genesis relationship. This finding is consistent with the recent analysis results of Wang et al. (2017), who noticed, by analyzing records of 1957–2016, that the WNP anticyclone occurs after a peak El Niño only for strong El Niño events rather than for the weak events. Due to the absence of the WNP anticyclonic anomalies in the weak or CP El Niño events, the negative OND ENSO-early TC genesis relationship can no longer sustain.

The results here have important implications for the TC seasonal forecast over the WNP. Distinguishing EP and CP ENSO and/or strong and weak ENSO events during the OND season may help to improve the early season TC genesis prediction. In addition, the anthropogenic forcing may shift the ENSO SST signals to the CP by enhancing the thermocline feedback in the CP (Yeh et al. 2009), which implies that the negative correlation may be further weakened under global warming scenarios. It should be noted that only the impacts of external forcing on ENSO behaviors can be inferred in the multi-model ensemble mean as the phase of internal-variability in projections is randomly distributed (Hawkins and Sutton 2009; Meehl et al. 2009). Therefore, the recovery of negative correlation after 2006 and the possible weakening correlation in global warming scenarios are not contradictory due to the absence of internal-variability in the constructed projection in warming scenarios. More investigation is required to explore this possibility by using the outputs of the current state-of-the-art models of the Earth's climate system.

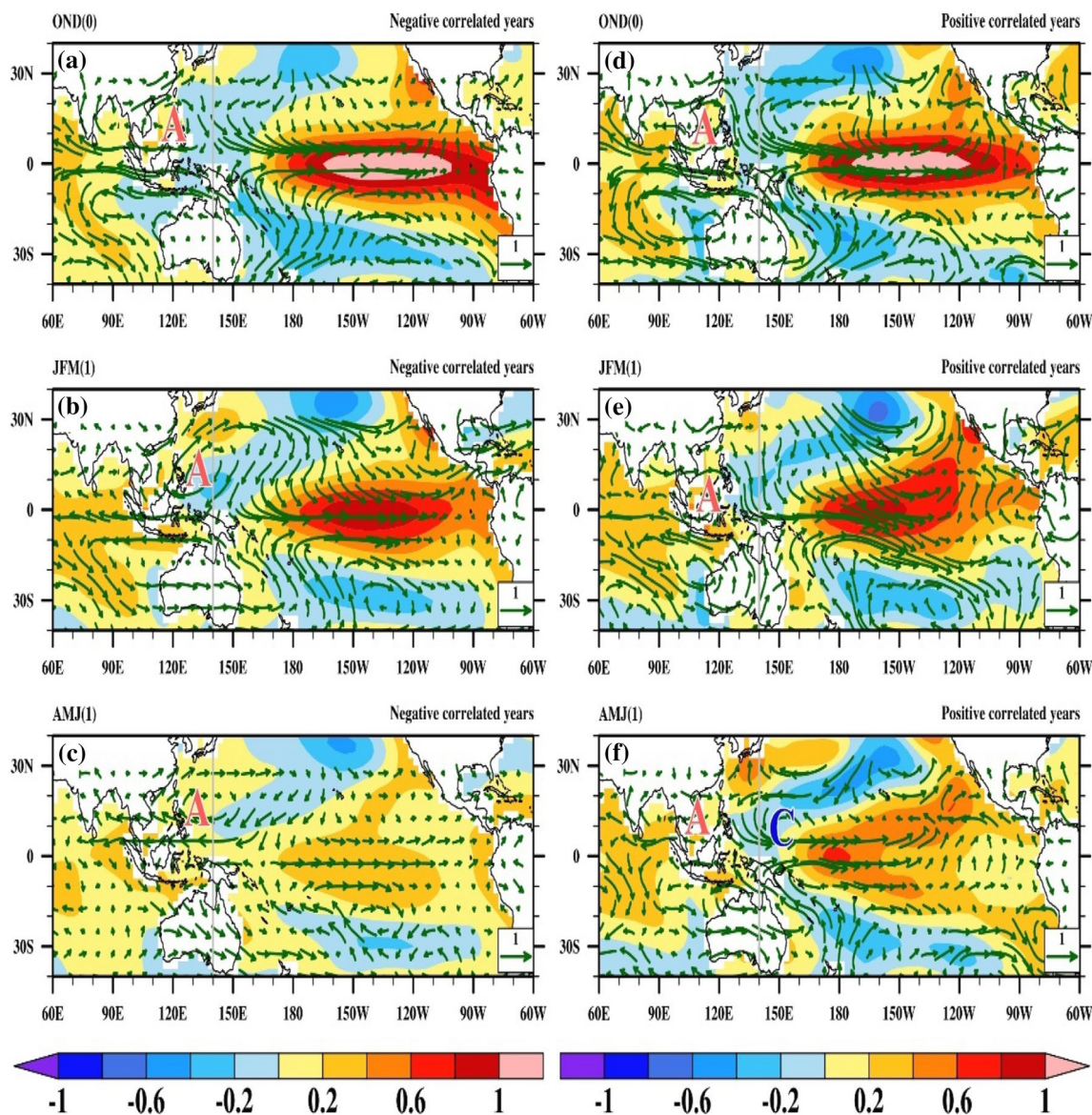


**Fig. 11** Seasonal evolutions from OND(0) to AMJ(1) of regressed SST (shading) and 850 hPa wind anomalies for negatively correlated years (a–c) and positively correlated years (d–f) with respect to OND Niño 3.4 index. The numerals in parentheses denote the ENSO devel-

oping (0) and decaying (1) years. The grey lines denote 140°E. A denotes the anti-cyclonic circulation and C denotes the cyclonic circulation

**Acknowledgements** This study is supported by the Atmosphere–Ocean Research Center (AORC). The AORC is partially funded by the Nanjing University of Information Science and Technology (NUIST). This research is jointly supported by the National Basic Research Program of China (Grant No. 2015CB452803), the National Natural Science Foundation of China (Grant Nos. 41420104002, 41730961, 41675051 and 41705060), the National Key Research and Development Program of China (Grant No. 2016YFA0600401), the Natural Science Foundation of Jiangsu Province (Grant No. BK20170941), the Startup Foundation for Introducing Talent of NUIST (Grant No. 2016r048), and the Priority Academic Program Development of Jiangsu Higher Education Institutions (PAPD). The authors also thank anonymous reviewers for the constructive comments that led to significant improvement of the original manuscript. This is the NUIST-Earth System Modeling Center

(ESMC) publication number 226, the School of Ocean and Earth Science and Technology (SOEST) publication number 10416, and the IPRC publication number 1328.

**References**

Ashok K, Behera SK, Rao SA, Weng H, Yamagata T (2007) El Niño Modoki and its possible teleconnection. *J Geophys Res.* <https://doi.org/10.1029/2006jc003798>  
 Briegel LM, Frank WM (1997) Large-scale influences on tropical cyclogenesis in the Western North

- Pacific. *Mon Weather Rev* 125:1397–1413. [https://doi.org/10.1175/1520-0493\(1997\)125<1397:LSIOTC>2.0.CO;2](https://doi.org/10.1175/1520-0493(1997)125<1397:LSIOTC>2.0.CO;2)
- Camargo SJ, Sobel AH (2005) Western North Pacific tropical cyclone intensity and ENSO. *J Clim* 18:2996–3006. <https://doi.org/10.1175/JCLI3457.1>
- Camargo SJ, Barnston AG, Klotzbach PJ, Landsea CW (2007) Seasonal tropical cyclone forecasts. *WMO Bull* 56:297–309
- Chan JCL (1985) Tropical cyclone activity in the northwest Pacific in relation to the El Niño/Southern Oscillation phenomenon. *Mon Weather Rev* 113:599–606
- Chan JCL (2000) Tropical cyclone activity over the western North Pacific associated with El Niño and La Niña events. *J Clim* 13:2960–2972. [https://doi.org/10.1175/1520-0442\(2000\)013<2960:TCAOTW>2.0.CO;2](https://doi.org/10.1175/1520-0442(2000)013<2960:TCAOTW>2.0.CO;2)
- Chan JCL (2005) Interannual and interdecadal variations of tropical cyclone activity over the western North Pacific. *Meteorol Atmos Phys* 89:143–152. <https://doi.org/10.1007/s00703-005-0126-y>
- Chan JC (2006) Comment on “Changes in tropical cyclone number, duration, and intensity in a warming environment. *Science* 311(80):1713. <https://doi.org/10.1126/science.1121522> (author reply 1713)
- Chan JCL, Shi J, Lam C-M (1998) Seasonal forecasting of tropical cyclone activity over the Western North Pacific and the South China Sea. *Weather Forecast* 13:997–1004. [https://doi.org/10.1175/1520-0434\(1998\)013<0997:SFOTCA>2.0.CO;2](https://doi.org/10.1175/1520-0434(1998)013<0997:SFOTCA>2.0.CO;2)
- Chan JCL, Shi J-E, Liu KS (2001) Improvements in the seasonal forecasting of tropical cyclone activity over the Western North Pacific. *Weather Forecast* 16:491–498. [https://doi.org/10.1175/1520-0434\(2001\)016<0491:IITFSO>2.0.CO;2](https://doi.org/10.1175/1520-0434(2001)016<0491:IITFSO>2.0.CO;2)
- Chen G, Tam C-Y (2010) Different impacts of two kinds of Pacific Ocean warming on tropical cyclone frequency over the western North Pacific. *Geophys Res Lett*. <https://doi.org/10.1029/2009g1041708>
- Chen T-C, Weng S-P, Yamazaki N, Kiehne S (1998) Interannual variation in the tropical cyclone formation over the western North Pacific. *Mon Weather Rev* 126:1080–1090
- Chia HH, Ropelewski CF (2002) The interannual variability in the genesis location of tropical cyclones in the northwest Pacific. *J Clim* 15:2934–2944
- Emanuel KA, Nolan DS (2004) Tropical cyclone activity and global climate. In: *Proceedings of 26th conference on hurricanes and tropical meteorology*. American Meteorological Society, Miami, FL, pp 240–241
- Gray WM (1968) Global view of the origin of tropical disturbances and storms. *Mon Weather Rev* 96:669–700
- Hawkins E, Sutton R (2009) The potential to narrow uncertainty in regional climate predictions. *Bull Am Meteorol Soc* 90:1095–1107. <https://doi.org/10.1175/2009BAMS2607.1>
- Hong C-C, Li Y-H, Li T, Lee M-Y (2011) Impacts of central Pacific and eastern Pacific El Niños on tropical cyclone tracks over the western North Pacific. *Geophys Res Lett*. <https://doi.org/10.1029/2011GL048821>
- Hsu P-C, Chu P-S, Murakami H, Zhao X (2014) An abrupt decrease in the late-season typhoon activity over the Western North Pacific\*. *J Clim* 27:4296–4312. <https://doi.org/10.1175/JCLI-D-13-00417.1>
- Huang B et al (2015) Extended reconstructed sea surface temperature version 4 (ERSST.v4). Part I: upgrades and intercomparisons. *J Clim* 28:911–930. <https://doi.org/10.1175/JCLI-D-14-00006.1>
- Kalnay E et al (1996) The NCEP/NCAR 40-year reanalysis project. *Bull Am Meteorol Soc* 77:437–471
- Kao HY, Yu JY (2009) Contrasting Eastern-Pacific and Central-Pacific types of ENSO. *J Clim* 22:615–632. <https://doi.org/10.1175/2008JCLI2309.1>
- Kim HM, Webster PJ, Curry JA (2009) Impact of shifting patterns of Pacific Ocean warming on North Atlantic tropical cyclones. *Science* (80-) 325:77–80. <https://doi.org/10.1126/science.1174062>
- Kim H-M, Webster PJ, Curry JA (2011) Modulation of North Pacific tropical cyclone activity by three phases of ENSO. *J Clim* 24:1839–1849. <https://doi.org/10.1175/2010JCLI3939.1>
- Kug J-S, Jin F-F, An S-I (2009) Two types of El Niño events: cold tongue El Niño and warm pool El Niño. *J Clim* 22:1499–1515. <https://doi.org/10.1175/2008jcli2624.1>
- Lander MA (1994) An exploratory analysis of the relationship between tropical storm formation in the Western North Pacific and ENSO. *Mon Weather Rev* 122:636–651. [https://doi.org/10.1175/1520-0493\(1994\)122<0636:AEAOTR>2.0.CO;2](https://doi.org/10.1175/1520-0493(1994)122<0636:AEAOTR>2.0.CO;2)
- Larkin NK, Harrison DE (2005) Global seasonal temperature and precipitation anomalies during El Niño autumn and winter. *Geophys Res Lett* 32:L16705. <https://doi.org/10.1029/2005GL022860>
- Lau N-C, Nath MJ (2003) Atmosphere–ocean variations in the Indo-Pacific sector during ENSO episodes. *J Clim* 16:3–20
- Lau N-C, Nath MJ, Wang H (2004) Simulations by a GFDL-GCM of ENSO related variability of the coupled atmosphere–ocean system in the East Asia monsoon region. In: C-P Chang (ed) *East Asian Monsoon*. World Scientific, Singapore, pp 271–300
- McGregor S, Timmermann A, Schneider N, Stuecker MF, England MH (2012) The effect of the South Pacific convergence zone on the termination of El Niño events and the Meridional asymmetry of ENSO\*. *J Clim* 25:5566–5586. <https://doi.org/10.1175/JCLI-D-11-00332.1>
- Meehl GA et al (2009) Decadal prediction. *Bull Am Meteorol Soc* 90:1467–1485. <https://doi.org/10.1175/2009bams2778.1>
- Meinen CS, McPhaden MJ (2000) Observations of warm water volume changes in the equatorial Pacific and their relationship to El Niño and La Niña. *J Clim* 13:3551–3559. [https://doi.org/10.1175/1520-0442\(2000\)013<3551:OOWWVC>2.0.CO;2](https://doi.org/10.1175/1520-0442(2000)013<3551:OOWWVC>2.0.CO;2)
- Murakami H, Wang B (2010) Future change of North Atlantic tropical cyclone tracks: projection by a 20-km-mesh global atmospheric model. *J Clim* 23:2699–2721. <https://doi.org/10.1175/2010JCLI3338.1>
- Okumura YM, Deser C (2010) Asymmetry in the duration of El Niño and La Niña. *J Clim* 23:5826–5843. <https://doi.org/10.1175/2010JCLI3592.1>
- Ritchie EA, Holland GJ (1999) Large-scale patterns associated with tropical cyclogenesis in the Western Pacific. *Mon Weather Rev* 127:2027–2043. [https://doi.org/10.1175/1520-0493\(1999\)127<2027:LSPAWT>2.0.CO;2](https://doi.org/10.1175/1520-0493(1999)127<2027:LSPAWT>2.0.CO;2)
- Wang B, Chan JCL (2002) How strong ENSO events affect tropical storm activity over the western North Pacific. *J Clim* 15:1643–1658. [https://doi.org/10.1175/1520-0442\(2002\)015<1643:HSE EAT>2.0.CO;2](https://doi.org/10.1175/1520-0442(2002)015<1643:HSE EAT>2.0.CO;2)
- Wang C, Wu L (2012) Tropical cyclone intensity change in the Western North Pacific: downscaling from IPCC AR4 experiments. *J Meteorol Soc Jpn* 90:223–233. <https://doi.org/10.2151/jmsj.2012-205>
- Wang C, Wu L (2015) Influence of future tropical cyclone track changes on their basin-wide intensity over the western North Pacific: downscaled CMIP5 projections. *Adv Atmos Sci* 32:613–623. <https://doi.org/10.1007/s00376-014-4105-4>
- Wang C, Wu L (2016) Interannual shift of the tropical upper-tropospheric trough and its influence on tropical cyclone formation over the Western North Pacific. *J Clim* 29:4203–4211. <https://doi.org/10.1175/JCLI-D-15-0653.1>
- Wang C, Wu L (2018a) Projection of North Pacific tropical upper-tropospheric trough in CMIP5 models: implications for changes in tropical cyclone formation locations. *J Clim* 31:761–774. <https://doi.org/10.1175/JCLI-D-17-0292.1>
- Wang C, Wu L (2018b) Future changes of the monsoon trough: sensitivity to sea surface temperature gradient and implications

- for tropical cyclone activity. *Earth's Futur.* <https://doi.org/10.1029/2018EF000858>
- Wang B, Zhang Q (2002) Pacific–East Asian teleconnection. Part II: how the Philippine sea anomalous anticyclone is established during El Niño development\*. *J Clim* 15, 3252–3265. [https://doi.org/10.1175/1520-0442\(2002\)015<3252:PEATPI>2.0.CO;2](https://doi.org/10.1175/1520-0442(2002)015<3252:PEATPI>2.0.CO;2)
- Wang B, Wu R, Fu X (2000) Pacific–East Asian teleconnection: how does ENSO affect East Asian climate? *J Clim* 13:1517–1536. [https://doi.org/10.1175/1520-0442\(2000\)013<1517:PEATHD>2.0.CO;2](https://doi.org/10.1175/1520-0442(2000)013<1517:PEATHD>2.0.CO;2)
- Wang B, Wu R, Li TIM (2003) Atmosphere–warm ocean interaction and its impacts on Asian–Australian monsoon variation\*. *J Clim* 16:1195–1211. [https://doi.org/10.1175/1520-0442\(2003\)16<1195:AOIAII>2.0.CO;2](https://doi.org/10.1175/1520-0442(2003)16<1195:AOIAII>2.0.CO;2)
- Wang B, Xiang B, Lee J-Y (2013a) Subtropical High predictability establishes a promising way for monsoon and tropical storm predictions. *Proc Natl Acad Sci* 110:2718–2722. <https://doi.org/10.1073/pnas.1214626110>
- Wang C, Li C, Mu M, Duan W (2013b) Seasonal modulations of different impacts of two types of ENSO events on tropical cyclone activity in the western North Pacific. *Clim Dyn* 40:2887–2902. <https://doi.org/10.1007/s00382-012-1434-9>
- Wang B, Li J, He Q (2017) Variable and robust East Asian monsoon rainfall response to El Niño over the past 60 years (1957–2016). *Adv Atmos Sci* 34:1235–1248. <https://doi.org/10.1007/s00376-017-7016-3>
- Wang C, Wu L, Zhao H, Cao J, Tian W (2018c) Is there a quiescent typhoon season over the western North Pacific following a strong El Niño event? *Int J Climatol.* <https://doi.org/10.1002/joc.5782>
- Weng H, Ashok K, Behera SK, Rao SA, Yamagata T (2007) Impacts of recent El Niño Modoki on dry/wet conditions in the Pacific rim during boreal summer. *Clim Dyn* 29:113–129. <https://doi.org/10.1007/s00382-007-0234-0>
- Weng H, Behera SK, Yamagata T (2009) Anomalous winter climate conditions in the Pacific rim during recent El Niño Modoki and El Niño events. *Clim Dyn* 32:663–674. <https://doi.org/10.1007/s00382-008-0394-6>
- Wilks DS (2011) *Statistical methods in the atmospheric sciences*. Academic Press, Oxford, p 676
- Wu L, Wang C, Wang B (2015) Westward shift of western North Pacific tropical cyclogenesis. *Geophys Res Lett* 42:1537–1542. <https://doi.org/10.1002/2015GL063450>
- Xiang B, Wang B, Li T (2013) A new paradigm for the predominance of standing Central Pacific warming after the late 1990s. *Clim Dyn* 41:327–340. <https://doi.org/10.1007/s00382-012-1427-8>
- Yeh S-W, Kug J-S, Dewitte B, Kwon M-H, Kirtman BP, Jin F-F (2009) El Niño in a changing climate. *Nature* 461:511–514. <https://doi.org/10.1038/nature08316>
- Zhan RF, Wang Y, Ying M (2012) Seasonal forecasts of tropical cyclone activity over the western North Pacific: a review. *Trop Cyclone Res Rev* 1:307–324. <https://doi.org/10.6057/2012TCRR03.07>
- Zhang Q, Wu L, Liu Q (2009) Tropical cyclone damages in China 1983–2006. *Bull Am Meteorol Soc* 90:489–495. <https://doi.org/10.1175/2008BAMS2631.1>
- Zhao H, Wu L, Zhou W (2011) Interannual changes of tropical cyclone intensity in the Western North Pacific. *J Meteorol Soc Jpn* 89:243–253. <https://doi.org/10.2151/jmsj.2011-305>